applied sciences

MDPI

Article

Cable Force Optimization of Cable-Stayed Bridge Based on Multiobjective Particle Swarm Optimization Algorithm with Mutation Operation and the Influence Matrix

Lifeng Wang [1,*], Ziwang Xiao [1], Min Li [1] and Ning Fu [2]

[1] School of Civil Engineering, Northeast Forestry University, Harbin 150006, China
[2] China Railway 22nd Bureau Group Corporation Limited, Beijing 100043, China
* Correspondence: lifengwang@nefu.edu.cn; Tel.: +86-18645065527

Abstract: To compensate the incapability of traditional cable force adjustment methods to automatically optimize cable forces, this paper proposes Midas/Civil and MATLAB as a structure calculator and a cable force optimizer, and external memory as a data transfer. Initial solutions from conventional methods can be optimized by internalizing the influence matrix into the multiobjective particle swarm optimization algorithm with mutation operation and constructing the mathematical model of cable force optimization, and then, a series of Pareto frontier solution sets are obtained. For the first time, fuzzy set theory is introduced for selecting Pareto presolution set for the optimization of cable-stayed bridges, to solve the final reasonable dead load state of bridges. By using this method, the peak vertical displacement of a main girder of the optimized cable-stayed bridge decreased from −11 mm to −6 mm, with a reduction of 45%. Before and after optimization, the difference of peak negative bending moment at the top of the pier was 34.8%, indicating that the main beam was more evenly stressed and the alignment was more reasonable.

Keywords: multiobjective particle swarm optimization; influence matrix; cable force optimization; reasonable finished status; fuzzy set theory

check for updates

Citation: Wang, L.; Xiao, Z.; Li, M.; Fu, N. Cable Force Optimization of Cable-Stayed Bridge Based on Multiobjective Particle Swarm Optimization Algorithm with Mutation Operation and the Influence Matrix. *Appl. Sci.* **2023**, *13*, 2611. https://doi.org/10.3390/app13042611

Academic Editors: Ichiro Ario, Yuki Chikahiro and Gakuho Watanabe

Received: 2 January 2023
Revised: 13 February 2023
Accepted: 15 February 2023
Published: 17 February 2023

1. Introduction

Nowadays, cable-stayed bridge structure accounts for a large proportion of modern bridge construction because of their beautiful shape and powerful crossing capacity. Compared with continuous girder bridge structures and rigid frame bridge structures, the advantage of cable-stayed bridge structures is that the distribution of its internal forces can be more uniform and reasonable by adjusting cable forces. Since the variation of cable force directly determines the internal force distribution of a whole bridge, the determination of reasonable cable forces and construction cable forces is the focus of cable-stayed bridge construction and its difficulty [1]. Specifically speaking, in the construction process of a cable-stayed bridge structure, it is necessary to stretch the cable several times in stages. The deformation and stress state of the bridge tower and main beam can be improved through the optimization of tension cable forces. Then, the reasonable state can be achieved by the reasonable bridge construction process within the allowable range of error.

The common methods to determine the reasonable bridge cable force include the zero-displacement method, the force balance method, the rigid supported continuous beam method, the minimum bending energy method, and the influence matrix method. Wang et al. [2], first proposed the zero-displacement method in 1993, which was used in order to determine the post-cable tension of cable-stayed bridges under dead load. Chen et al. [3]. proposed a new method to determine the cable force of cable-stayed bridges using the idea of force balance. Compared with the zero-displacement method, this method is easier to understand and more efficient. All other traditional methods have their own scope of application. For instance, the rigid supported continuous beam method takes the bending moment of the main beam as the control objective, which is simpler and more intuitive, and can overcome the defect that the zero-displacement method cannot deal with the local unreasonable bending moment of the main beam. However, the method does not consider the stress state of the bridge tower.

It is worth noting that a non-negligible problem is that the traditional cable force adjustment method also cannot realize automatic optimization of the cable force in the adjustment process [4]. The traditional method of determining the cable force of a single formed bridge only reflects the variation between the corresponding structural responses of the structure due to its action of constant load and so on. This is not only subjective, but also lacks rigorous mathematical calculations. For example, the influence matrix method describes the functional relationship between the adjustable variables and the target conditions, which only expresses a law of the structural mechanics system, and it does not obtain the optimal solution by itself [5]. To overcome this deficiency, an increasing number of scholars have introduced swarm intelligence algorithms into the cable force optimization process of cable-stayed bridges in the past decade [6]. The phenomenon continues to grow, which means that the cable force optimization problem of the swarm intelligence algorithms has attracted more and more scholars' interest in recent years, and has gradually become a research hotspot.

Nowadays, particle swarm optimization (PSO) and genetic algorithms are mainly used in cable force optimization of cable-stayed bridges [7]. Since the particle swarm optimization algorithm was proposed, it has been widely used in various fields because of its many advantages, such as easy-to-understand principle, fast convergence speed, easy implementation of algorithm code, and small number of parameters. Wu et al. [8] applied a genetic algorithm to cable force optimization of cable-stayed bridges. In this paper, a stepwise algorithm is proposed to determine the reasonable completion state of the hybrid girder cable-stayed bridge, and the improved genetic algorithm is used in order to optimize the cable force of the hybrid girder cable-stayed bridge of Jiujiang No. 2 Bridge under dead load. Compared with the traditional method of determining the cable force, this algorithm avoids the later work of cable adjustment. Arellano et al. [9] used the evolutionary nondominated sorted genetic algorithm (NSGA) to solve the multiobjective optimization problem of multispan cable-stayed bridges. The genetic algorithm only takes a few seconds to find the nondominated solution set comprising the Pareto front.

In addition, many scholars have extended this kind of method to the field of bridge structure optimization design, which makes its application scope more extensive. The latest cable force optimization algorithms suitable for cable-stayed bridges have been increasingly paid attention by scholars. Feng et al. [10] proposed an optimal design method for cable-stayed bridges by combining an influence matrix method with genetic algorithm and applied it to the preliminary design of the cable-stayed bridge with two towers and two cable planes located in Ferrara, Italy. At present, the main method of introducing the swarm intelligence optimization algorithm to realize cable force optimization of cable-stayed bridges is based on the interaction between programming language and large general design software. Zhu et al. [11] used a multipopulation genetic algorithm to optimize the cable force of long-span cable-stayed bridges under reasonable completion state by establishing the parametric analysis model with APDL (Ansys Parametric Design Language). The research proves the feasibility and validity of the multipopulation genetic algorithm in the optimization of the cable force of long-span cable-stayed bridges considering nonlinearity. It is undeniable that ANSYS is an excellent fine analysis software. For example, scholars such as Birinci et al. [12] have used ANSYS for fine analysis and obtained satisfactory results. However, Ansys, as large general finite element design software, is still lacking in the professional bridge module compared with the special software for bridges. Liu et al. [13] and Zhang et al. [14] developed a program for automatic optimization of cable forces in Python language based on FBR_CAL_SUO, a planar rod mechanical calculation software developed by Professor Li Chuanxi of Changsha University of Technology. The particle swarm intelligent optimization algorithm and the reasonable state of cable-stayed bridge proposed by Zhang Yuping are the theoretical bases. The automatic optimization of cable-stayed bridge cable forces and the determination of reasonable state are finally completed.

However, the number of users of the finite element software is not substantial, and the ultimate choice of the most optimal solution for the Pareto front solution sets depends largely on individual judgment. Atmaca et al. [15,16] write code in MATLAB based on the OAPI (Open Application Programming Interface) function of SAP2000 to realize the interactive use of MATLAB and SAP2000. Finally, the Jaya optimization algorithm was successfully applied to optimize the tension forces of a single-tower cable-stayed bridge and a multitower cable-stayed bridge, and the internal forces and alignment of the cable-stayed bridge were still more reasonable under the premise that the total weight of the cable was reduced from the initial basis. However, the current problem is that SAP2000 has separated its bridge module from SAP2000V15.1.0/1, which means that SAP2000 software itself in the field of bridge application does not have the characteristics of further promotion, even if its OAPI function is very powerful. Therefore, the introduction of the particle swarm optimization (PSO) algorithm into cable force optimization of cable-stayed bridges needs to solve the problem that it is easy to fall into local optimum theoretically on the one hand, and to be more rigorous in determining the final optimization solution at the same time. Furthermore, it is necessary to solve the problem that the bridge special software cannot integrate with the algorithm without an API function.

Therefore, this paper proposes a method to optimize the stress of cable-stayed bridges by using the commonly used professional bridge design software Midas/Civil and the programming software MATLAB. This makes it unnecessary to rely on API interface when using the step-by-step optimization method of traditional optimization algorithm and then swarm intelligence optimization algorithm to optimize cable force. At the same time, the mutation operation is introduced to improve the multiobjective particle swarm optimization algorithm in the MATLAB platform to improve its performance towards local optimization, and it is combined with the influence matrix to make up for the lack of this aspect in the research. Finally, in the optimal solution selection of the Pareto front end solution set, the fuzzy set theory is introduced into the field of cable-stayed bridge force optimization for the first time to further select the Pareto front solution set to obtain the optimal cable force.

2. Optimization Methods and Design Procedure

2.1. SOM Optimization Method

This paper proposes a structural calculator and optimizer method (SOM) based on professional bridge software and programming software to optimize cable force by seeking external data storage and transfer media. The selection of bridge-specific software for the structural calculator ensures its broad applicability and professionalism. The selection of programming software as the optimizer allows organic integration with the swarm intelligence algorithm. However, the optimizer itself does not have the function to realize the synergy between mathematics and mechanics, so it is necessary to consider introducing the concept of mechanics into the optimizer. The influence matrix method can well accomplish this connection between mathematics and mechanics. Based on the concept of generalized influence matrix, Xiao et al. [5] derived the influence matrix method for cable force optimization of cable-stayed bridges. Under the condition that the structure meets the principle of linear superposition, the change of internal force (such as cable force) of the structure has the following relationship with the structural response:

$$[I]\{X\} = \{C\} \tag{1}$$

where $[I]$ is the influence matrix, and $\{X\}$ is the adjustment vector, which refers to the column vector composed of n independent elements specified in the structure that can be adjusted to change the adjustment vector. $\{C\}$ is the regulated vector, which refers to the column vector composed of m $(m > n)$ independent elements on the cross section of the structure, generally referring to the structural response of internal force, stress, or displacement of the cross section.

It is assumed that we have obtained a set of relatively reasonable cable force values $\{X_1\}$ and the corresponding vertical displacement of main beam $\{C_0\}$ for cable-stayed bridges according to traditional methods (the response of other structures follow the same principle). The influence matrix of the cable force corresponding to the vertical displacement of the main beam is noted as $[I_y]$. When the change of cable force value $\{\Delta X\}$ becomes $\{X_1\}$, the change of the vertical displacement of the main beam is denoted as $\{\Delta C\}$ and becomes $\{C_1\}$. When the span of a cable-stayed bridge is small and the structure is under elastic stress, the condition of the linear superposition principle is satisfied. At this point there is the following quantitative relationship:

$$[I_y]\{\Delta X\} = \{\Delta C\} \tag{2}$$

also known as

$$[I_C]\{X_1 - X_0\} = \{C_1 - C_0\} \tag{3}$$

By incorporating the above Equation (3) into the optimizer, the corresponding vertical displacement of the main beam can be obtained from the initial values of the cable force and the vertical displacement of the main beam when the position of the particle is updated (either by a regular update or by variation operation). Then, the objective function related to the vertical displacement of the main beam can be solved to evaluate the particles. It is worth noting that the premise of using the influence matrix method is that the response of the structure before and after the cable force adjustment satisfies the linear superposition principle, so the influence matrix is built into the optimizer in the field of cable force adjustment of small- and medium-span cable-stayed bridges to perform better. The primary roles of the cable force optimizer, the structure calculator, and the various parts of the data transfer medium are shown in Figure 1. The intelligent optimization algorithm uses particle swarm optimization, which has been proven to have excellent performance in cable force optimization. However, it needs to be further improved to optimize its performance.

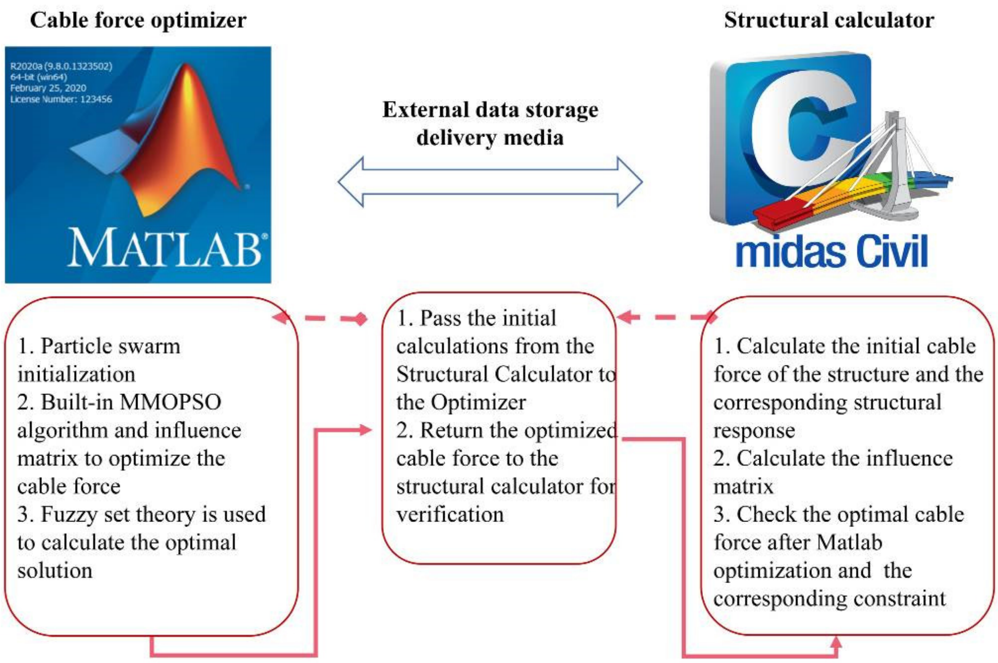

Figure 1. Collaboration between Midas/Civil and MATLAB.

2.2. Principle of Particle Swarm Optimization Algorithm

Particle swarm optimization proposed by Kennedy et al. [17] is a kind of intelligent optimization algorithm formed by simulating the intelligent behavior of bird foraging and so on. The initial displacement and velocity of everyone are randomly generated within a certain range. At the same time, in the process of searching for the optimal solution, each particle should not only carry on the next search according to the existing information, but also pay attention to its own experience and draw on the information of its peers to find the optimal solution. Figure 2 shows the optimal search process for population particles in the search space.

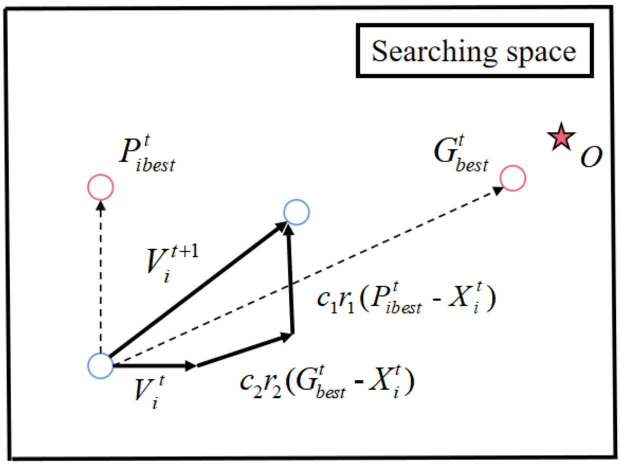

Figure 2. Optimization process of particles in search space.

In Figure 2, O represents the global optimal position, c_1 and c_2 denote the acceleration constants, r_1 and r_2 are two random numbers within the range of [0, 1], and X_i^t and V_i^t (multidimensional vectors), respectively, represent the spatial position and flight velocity of the particle swarm after tth iterations. P^t_{ibest} and G^t_{best} represent the individual optimal position and the global historical optimal position mastered by the ith particle, and the subscript i represents the ith particle. The speed and position update formula for the next optimization based on the individual historical optimal value and global optimal value is:

$$V_i^{i+1} = V_i^i + c_1r_1(P^t_{ibestj} - X_i^t) + c_2r_2(G^t_{best} - X_i^t) \tag{4}$$

$$X_i^{i+1} = X_i^i + V_i^{t+1} \tag{5}$$

2.2.1. Multiobjective Particle Swarm Optimization Algorithm with Mutation Operation

Limited by the search method, standard particle swarm algorithms tend to fall into local optimal solutions by incomplete global search. To avoid this situation, a variational operation is added to expand the search range during the optimization process [18]. The specific idea of the mutation strategy adopted in this paper is to divide the whole population into three parts equally. The first part retains the original characteristics of the particles, i.e., lets them keep their original flight state, to ensure that the particles in the population retain at least 1/3 of the initial population information. The second part randomly selects individuals for uniform mutation according to a certain proportion. Uniform variation means that the proportion of the variation does not change with the increase of population optimization generations. The third part of the nonuniform variation is used to simulate the phenomenon that as the number of population generations increases, the particles will gradually gather around the optimal solution when the global search is completed. In this case, it is better to reduce the proportion of variation of particles in order to avoid finding the optimal global solution and then abandoning it. The multiobjective particle swarm optimization algorithm with mutation operation is called the M-MOPSO algorithm. The flowchart of the M-MOPSO algorithm is shown in Figure 3. For multiobjective optimization theory, the final optimization result is a set of solutions rather than a single optimal solution, called the Pareto front solution.

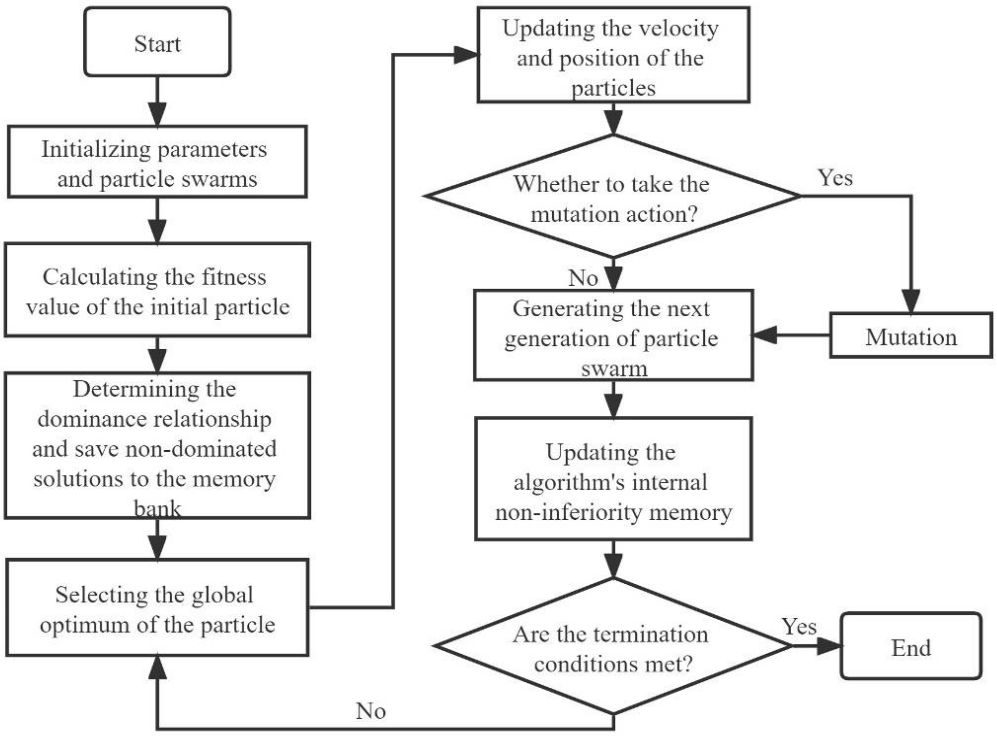

Figure 3. Flowchart of M-MOPSO algorithm.

2.2.2. Algorithm Test

The classic multiobjective benchmark function test set ZDT test function was selected to test the M-MOPSO algorithm. The classical algorithm NSGA-II was used for comparative analysis. The selected ZDT test functions include ZDT1, ZDT2, ZDT3, and ZDT6 [19]. Each test function represents the characteristic of different kinds of multiobjective functions, including convex front solution, concave front solution, and discontinuous front solution set. The decision variables of test function ZDT1, ZDT2, and ZDT3 were set to 30 dimensions. The decision variable for the test function ZDT6 was set to 10 dimensions. M-MOPSO algorithm parameters were set at population size of 200, external file size of 100, and maximum iteration number of 500, and all comparator-algorithm-related parameters were set according to references. The NSGA-II algorithm was set to the same population size, external file size, and maximum number of iterations. Test results were paired with classical NSGA-II algorithm solutions and real Pareto curves, as shown in Figure 4.

In Figure 4, the optimal results of the M-MOPSO algorithm for test functions are consistent with the real noninferior forward solution sets. The solution obtained for the ZDT6 function is better than that obtained by the NSGA-II algorithm. In terms of distribution, the M-MOPSO algorithm also performed well, and optimized results were evenly distributed. Whether convergent or distributive, multiobjective particle swarm algorithm with variable operation has obvious advantages in multiobjective problem and is an effective algorithm for multiobjective optimization.

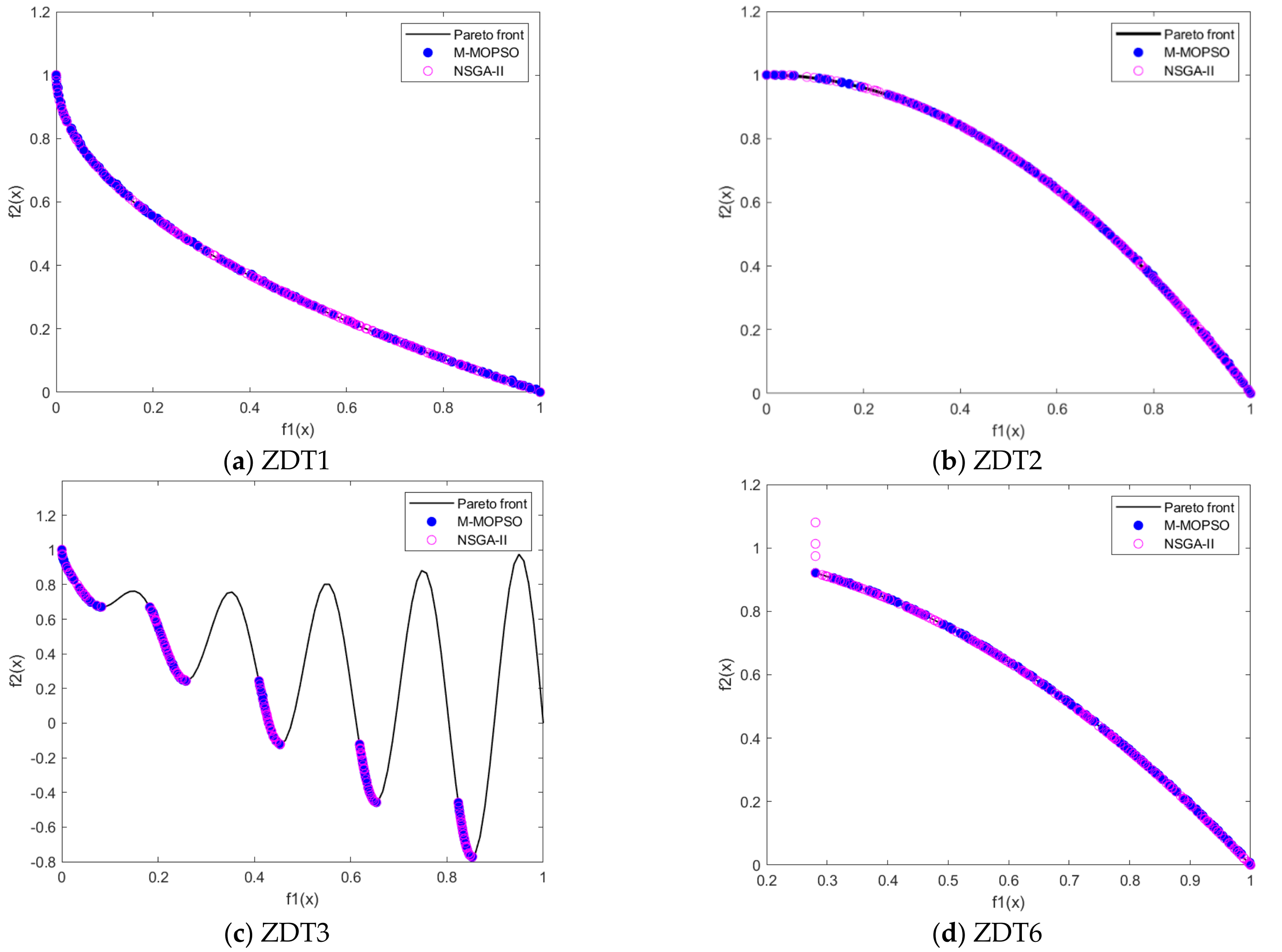

Figure 4. Comparison of Pareto front solution sets for the test functions.

2.2.3. Optimization Procedure

After calculating the initial state of cable force by traditional methods, the optimal design process of cable-stayed cable by SOM is as follows:

(1) The main program of the M-MOPSO algorithm in MATLAB is established and control parameters of particle swarm are input.
(2) The influence matrix is solved and built into the main algorithm program.
(3) The initial cable forces and constraints obtained by conventional methods initialize the particle swarm and update the corresponding structural response using the built-in influence matrix. The fitness value of the target function is calculated, and the particles are evaluated accordingly. The excellent particles are temporarily stored in a nondominant solution set.
(4) The velocity of particles is updated based on their evaluation. Variation is also performed from the particles selected in the proportions. The structural response, adaptive function, and particle evaluation are updated again using the built-in influence matrix.
(5) We judge whether the conditions for termination have been met and, if so, we terminated. Otherwise, we return to renew particle location and velocity to produce the next generation of population.
(6) Steps (4) and (5) are repeated until the Pareto front solution set of the cable force is obtained.

The optimization flow chart shown in Figure 5 summarizes all the above optimization steps.

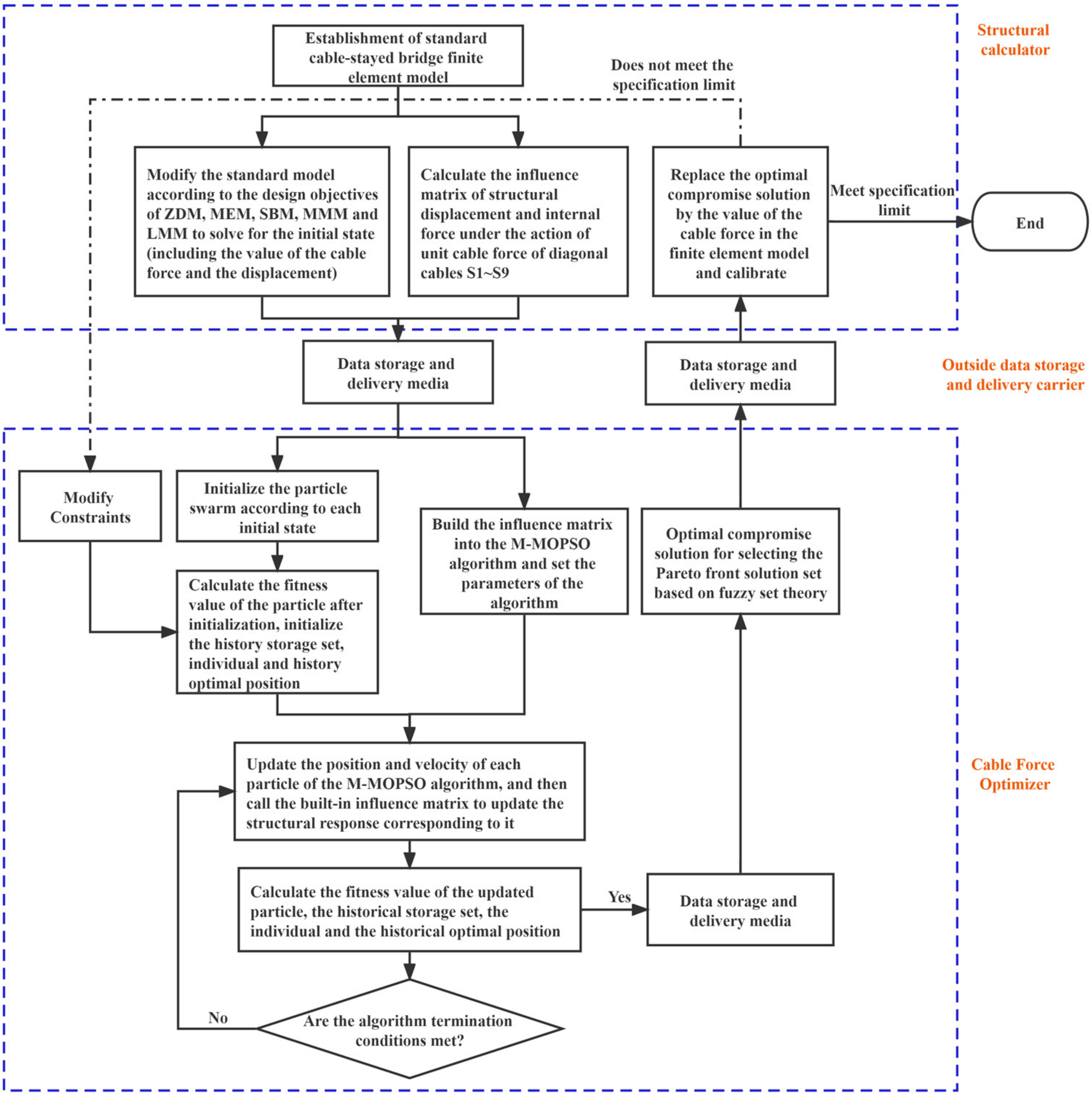

Figure 5. Flow chart of cable force optimization of SOM.

3. Mathematical Model of Cable Force Optimization

3.1. Design Variables

The most important feature of cable-stayed bridges compared with continuous girder bridges, rigid bridges, and arch bridges is that the internal force distribution can be adjusted by the cable force. Therefore, the cable force is used as the design variable of the optimization model. A set of design vectors in particle swarm optimization is a set of potential solutions for the particles being optimized. Its vector form is as follows:

$$T = [T_1, T_2, \ldots, T_n] \tag{6}$$

where T_i is the initial cable force value of the ith cable, and n is the number of design variables. If the cables are symmetrically arranged along the longitudinal bridge with respect to the bridge tower, then the design variable can be the force value of the unilateral cable. The number of design variables is taken as half of the total number of stay cables. If the cables along the longitudinal bridge are asymmetrically arranged with respect to the bridge tower, then the design variable should take all the cable force values.

3.2. Objective Function

At present, the accepted principle for determining the reasonable completion state of cable-stayed bridge structure is [20]:

(1) To maintain the vertical state of the bridge when the bridge is formed, and to reduce the horizontal displacement and meet the limit requirements without excessive local bending moment at the base of the bridge tower.
(2) To maintain the horizontal state of the girder when forming a bridge, to reduce its vertical displacement and to meet the limit value.
(3) To ensure the cable force distribution is uniform, which means that the cable force is positively correlated with the length of the cable itself.
(4) To induce no negative force at the support.

In the above principles, (1) and (2) are essentially constraints on the distribution and alignment of internal forces in the bridge state of members. The reasonable completion of the bridge state requires smooth alignment of pylons and main beams, uniform distribution of internal forces, and no excessive local stress. For the optimization objective of the main beam, the most common objective function can be the minimum bending energy of the main beam [21–23]. However, this is more applicable to equal-section beams. Since the equal-section beam has a fixed value of the flexural stiffness EI, the continuous main beam can be discretized and then solved using methods such as the influence matrix. For variable-section beams, this objective function is not applicable. Therefore, other objective functions must be sought. The main consideration is that the displacements of the beam and the main tower can reflect the bending of the main beam and the main tower to some extent, and considering that the displacement has positive and negative values, the vertical displacement of the control node of the main beam and the horizontal displacement of the control node of the bridge tower can be taken as the objective function. Chen et al. [24] used the sum of the arithmetic square root of the vertical displacement of the main beam and the vertical displacement of the bridge tower as the objective function. However, the different ranges of variation of main girder and tower displacements are not reflected in it. In order to distinguish the influence weights of the bridge tower and main beam on the objective function, the main objective function is finally determined as follows:

$$D = D_1 + D_2 = \lambda\sqrt{(x_1^2 + x_2^2 + \ldots + x_p^2)} + \sqrt{(y_1^2 + y_2^2 + \ldots + y_q^2)} \quad (7)$$

where $x_i(i = 1, 2, \ldots, p)$ is the horizontal displacement of the control node of the bridge tower, n is the number of horizontal control nodes, $y_i(i = 1, 2, \ldots, q)$ is the vertical displacement of the control node of the main beam, m is the number of vertical control nodes, and λ reflects that the weight of the horizontal displacement of the main tower is different from the vertical displacement of the main beam.

Principle (3) is that for the cable force, the cable force distribution generally increases from the main tower to both ends (short cables to long cables). Small local jump variations in individual cable force values are allowed. Take the first pair of cable forces on both sides of the main tower and the tail cable forces as examples. The positive correlation between the cable force and its length can be explained by the fact that the longer the cable, the higher the value of the cable force, and vice versa, the lower the value. The closer the set of cable forces distributed per unit length of each cable, the more uniform the cable force distribution of the cable system. This relation is only mathematically valid because this set degree has no physical meaning and is different from the set degree of axial force in material mechanics.

According to the above analysis, the objective function of cable force can be the range of the set degree of cable force per unit length:

$$R = R_{\max} - R_{\min} \quad (8)$$

$$R_{\max} = \max\{R_1, R_2, \ldots, R_n\} \quad (9)$$

$$R_{\min} = \min\{R_1, R_2, \ldots, R_n\} \quad (10)$$

$$R_i = \frac{T_i}{L_i}, i = 1, 2, \ldots, n \quad (11)$$

where R_i is the set degree of cable force of the cable with unit length, L_i is the length of the ith cable, $R_{\max}$ and $R_{\min}$ are the maximum and minimum values of cable force concentration, respectively.

3.3. Constraints Function

The constraint of the objective function should be that the stress of the bridge tower and main beam meet the allowable value of the code. The cable force should not exceed the safety factor required by the code. Specifically, it can be expressed as:

$$T_{i\min} \le T_i \le T_{i\max}, i = 1, 2, \ldots, n \quad (12)$$

$$\sigma_{i\min} \le \sigma_j \le \sigma_{i\max}, j = 1, 2, \ldots, s \quad (13)$$

where $T_{i\min}$ and $T_{i\max}$ are the upper and lower limits of the ith cable stay force. In this paper, the upper and lower limits are set as $1.3T_0$ and $0.7T_0$ (T_0 is the initial state cable force value calculated by the conventional method). $\sigma_{i\min}$ and $\sigma_{i\max}$ are, respectively, the upper and lower limits of the ith control section stress, and s is the number of stress points.

3.4. Mathematical Model

After determining the objective function and corresponding constraints, the optimization model of the cable force can be expressed as follows:

$$\begin{cases} \min f = [\min D, \min R] = [\min f_1, \min f_2] \\ s.t. g_w(\sigma_j, T_i) \le 0, w = 1, 2, \ldots, \varepsilon \end{cases} \quad (14)$$

where f is the objective function, including the objective term D of the horizontal displacement of the bridge tower and the vertical displacement of the main beam, R is the range of cable force concentration per unit length, $g_w(\sigma_j, T_i)$ is the unified form of constraints, and ε is the number of constraints.

3.5. The Pareto Front Solution Sets

In multiobjective optimization theory, the final optimization result is a set of solutions rather than a single optimal solution. This is the result of the mutual constraints between the objective functions. In a multiobjective optimization process, individual 1 is said to dominate individual 2 if at least one objective of individual 1 has a better fitness value than individual 2, and all objectives of individual 1 have a fitness value no worse than that of individual 2. If, as shown in Figure 6, $f_1(A) < f_1(B)$ and $f_2(A) > f_2(B)$, individuals A and B do not constitute a dominant relationship. Obviously, individuals A and B have dominance relations for C. Individuals in blue have dominance relations for all individuals in black. In the M-MOPSO algorithm, by defining an external storage set where the nondominated solutions in the iterative history are stored, a set of solutions (Pareto front solution set) that are not dominated by each other is obtained when the algorithm reaches the termination condition. In addition, the judgment of the crowding distance of the neighboring individuals of individual i is added to the selection of individuals within the Pareto solution set, as shown in Figure 7. Such a choice can avoid becoming trapped in a local optimum while expanding the search range.

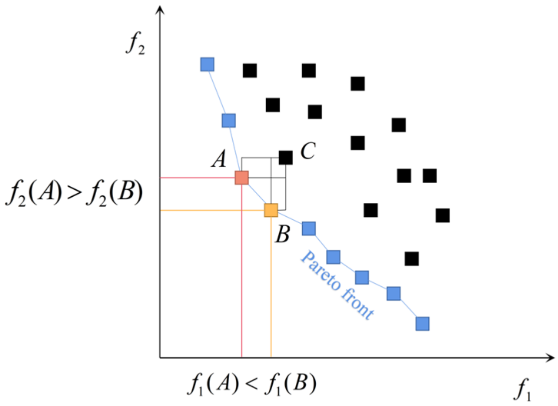

Figure 6. Dominance relationships among individuals.

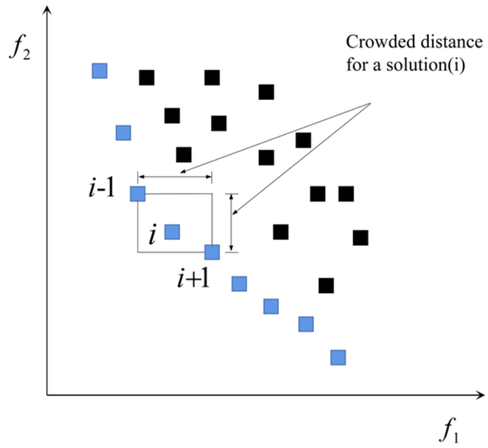

Figure 7. Crowding distance.

4. Result and Analysis—A Case Study

The cable-stayed T-frame composite bridge of the Nanxi River on the high-speed railway from Hangzhou to Wenzhou in Zhejiang Province of China is selected as an engineering case. The span composition of the main bridge of Nanxi River Bridge is (120 + 120) m, with a total length of 241.5 m. Prestressed concrete variable section box girders were used, with straight webs of single box and double-chamber cross section. Each end of the main girder has a straight section of 12.25 m long, followed by a variable section height of 104.5 m: the height of the girder varies parabolically from 5.8 m to 11.0 m. The top slab and bottom slab of the box girder are 14.0 m and 12.0 m, respectively. The tower is a double-column tower with a height of 35.0 m with the No. 0 section of the main beam. The cables are single-wire coated with epoxy-coated steel strand cables and a space double-cable plane system. The stay cables are numbered from S1 to S9 from the bridge tower to both sides. The cable distance on the beam is 8.0 m, and the cable distance on the tower is 1.0 m. The cable saddle on the tower is passed by a split-wire pipe and anchored at the beam end. The main pier adopts a hollow box section and the foundation is a bored pile foundation. The overall layout of the bridge type and the symmetry plane of the bridge tower are shown in Figure 8.

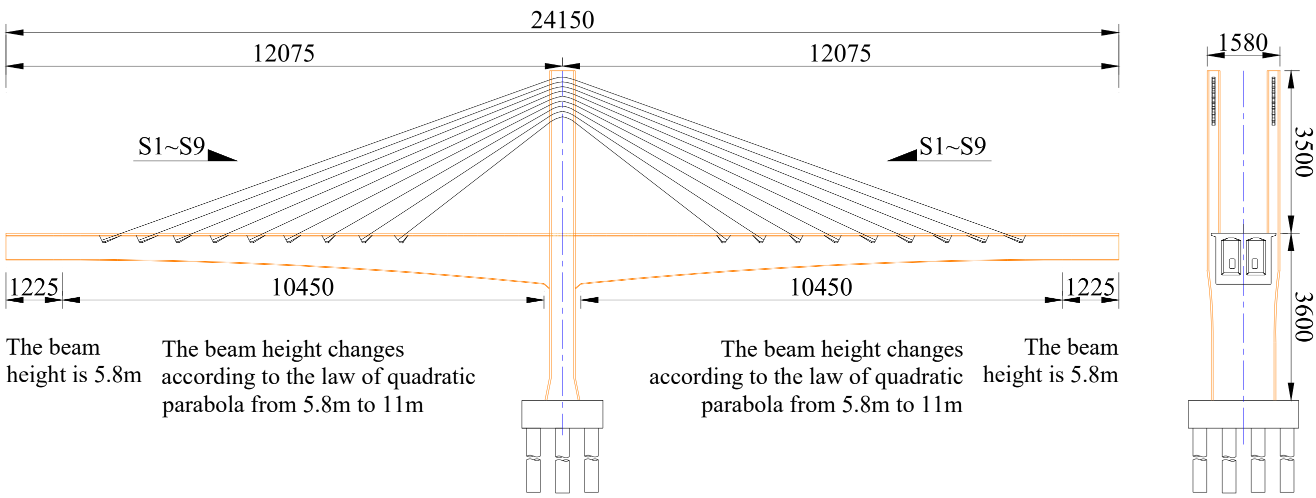

Figure 8. General layout of Nanxi River cable stayed T-frame bridge (unit: cm).

4.1. Numerical Model

The whole Nanxi River Bridge is discredited into 220 nodes and 180 elements, and the standard finite element model is established in Midas/Civil. The so-called standard model is a complete bridge model with acting dead weight and two-phase dead load. The spatial beam unit is used to simulate the main girders, piers, and towers. The truss unit is used to simulate the diagonal cables. Nanxi River Bridge is a single-tower cable-stayed bridge with tower and beam consolidation. The properties of the structural members are shown in Table 1 and the boundary conditions are shown in the following Table 2. The parameters in Table 1 are from the Code for Design of Highway Reinforced Concrete and Prestressed Concrete Bridges and Culverts (JTG 3382-2018). The connections between the tower and the main beam, between the main beam and the stay cable nodes, and between the tower and the stay cable nodes simulate coupling through rigid connections with "master–slave constraints".

Table 1. Properties of the structural members.

Position	Material	Material Type	Element Type	Elasticity Modulus (MPa)	Density (kg/m^3)	Poisson's Ratio
Main girder	Concrete	C60	beam	3.60×10^4	2500	0.2
Tower (above bridge deck)	Concrete	C50	beam	3.45×10^4	2500	0.2
Tower (under bridge deck)	Concrete	C60	beam	3.60×10^4	2500	0.2
Main pier	Concrete	C50	beam	3.45×10^4	2500	0.2
Stayed cable	Steel strand	Strand 1860	Truss	1.95×10^5	7850	0.3

Table 2. Boundary conditions in the FE model of the structural members.

Position	Dx	Dy	Dz	Rx	Ry	Rz
Bottom of the tower	Fixed	Fixed	Fixed	Fixed	Fixed	Fixed
Bottom of the pier	Fixed	Fixed	Fixed	Fixed	Fixed	Fixed
Intersection node between girder and tower	Free	Coupled	Coupled	Coupled	Free	Free
Intersection node between girder and pier	Free	Coupled	Coupled	Coupled	Free	Free
Intersection node between cable and tower	Coupled	Coupled	Coupled	Coupled	Coupled	Coupled
Intersection node between cable and girder	Coupled	Coupled	Coupled	Coupled	Coupled	Coupled
Beam end	Free	Fixed	Free	Fixed	Free	Fixed

Initializing the population and establishing the search space may have a certain impact on the results, then five finite element models are firstly established in the structure calculator. The zero-displacement method, the rigid supported continuous beam method, and minimum bending energy method are used to determine a initial state without cable force optimization. The above three methods establish different finite element models based on the standard model for calculating the initial bridge state. The standard calculation model is shown in Figure 9.

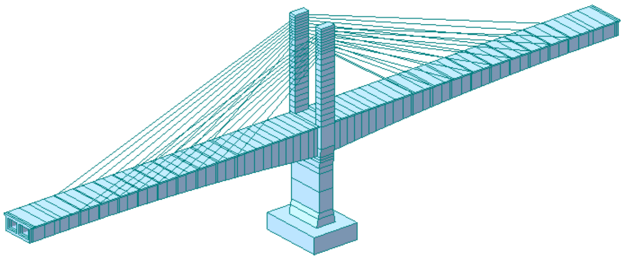

Figure 9. Standard finite element model of Nanxi River Bridge.

Considering the span of Nanxi River Bridge is (120 + 120) m, the sag effect of the cable is considered when modeling the cable by the equivalent truss element whose elastic modulus is modified by Ernst's formula (1965). Ernst's correction formula is as follows:

$$E_{eq} = \frac{E_0}{1 + \frac{(\gamma S \cos \alpha)^2 E_0}{12\sigma^3}} \quad (15)$$

where E_0 is the original elastic modulus of the cable (kPa). $\gamma = \frac{\text{Heavy material per cable and protective structure}}{\text{Area of cable sec tion}}$ is the gravity force per unit length of the cable (kN/m), S is the cable length, α is the angle between the cable and the horizontal line (°), and σ is the cable stress (kPa).

4.1.1. The Initial State

According to the different purposes of controlling the parameters of Nanxi River Bridge under the action of dead load, five preliminary calculation ideas are divided into the following through several trial calculations.

(1) The main beam of Nanxi River bridge was equivalent to a multispan continuous beam with multipoint elastic support. The vertical component of the cable force was balanced with the elastic support in the vertical direction. This goal could be realized by the simple beam method (SBM).
(2) The bending energy of the main beam was minimized, which could be achieved by the minimum bending energy method (MEM).
(3) The vertical displacement between the cable and the anchor point of the main beam was constrained to be between −20 mm and 20 mm, which can be achieved by the zero-displacement method (ZDM).
(4) The minimizing maximum bending moment (MMM) of the main beam is limited. The value was kept within the range of −180,000~200,000 kN.m. Yue Feng [10] used to limit the sum of the maximum bending moment values of the main beam and the main tower when studying the cable force optimization of a cable-stayed bridge with two towers and three spans. Considering the symmetry of Nanxi River Bridge, this paper only sets the limit value for the maximum bending moment of the main beam.
(5) Limiting the initial value of the pretension forces (PTF) of the cable was to ensure the uniformity of the cable force (limiting force method, LFM). In this paper, the initial PTF was uniformly set as 7000 kN, which was an integer value around the median cable force determined by several trial calculations. When determining the initial value, the cable force in working conditions 2~4 was set to the same values of 2000 kN, 2250 kN, and 2500 kN respectively by some scholars [22], making the consideration more abundant.

The initial state of Nanxi River Bridge obtained by calculating the above targets is shown in Figure 10a–c.

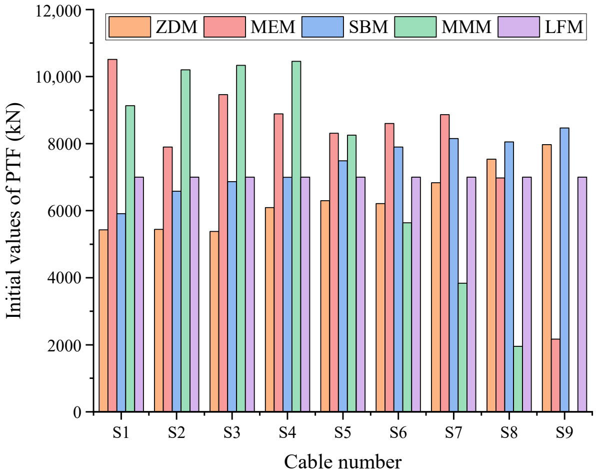

(**a**) Initial value of the pretension forces

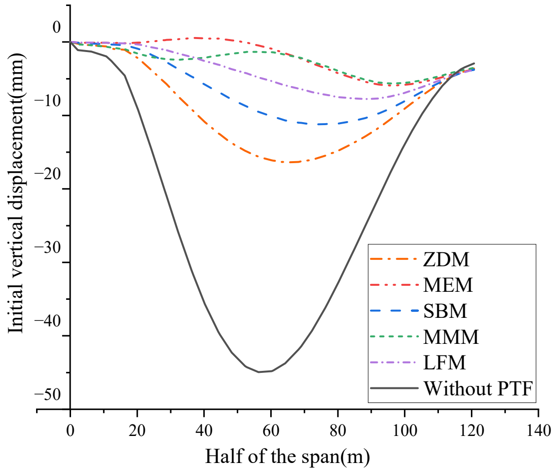

(**b**) Vertical displacement of main beam

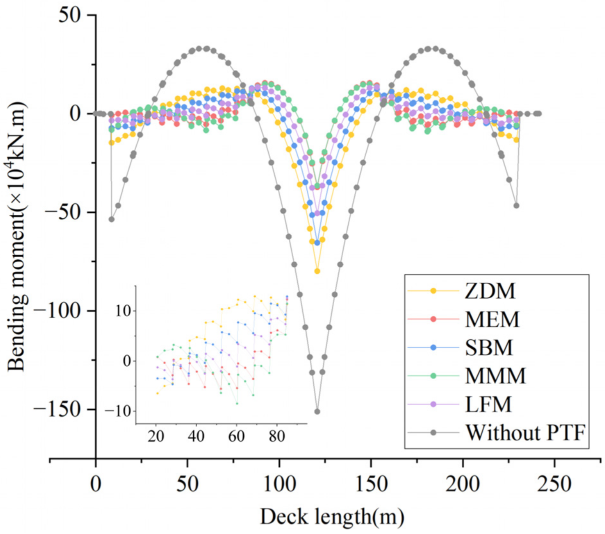

(**c**) Bending moment of main beam

Figure 10. Structural response of cable-stayed bridge in the initial state calculated by different methods.

Figure 10a illustrates that the cable force calculated by ZDM and SBM increases gradually with the increase of cable length, indicating that the cable force distribution of both is more uniform. The cable forces calculated by the ZDM method are 5431 kN, 5440 kN, and 5379 kN between S1 and S3, respectively. There is partial unevenness of the value of cable force. The SBM method also shows this phenomenon between the cable force values numbered S7 to S9, which is allowed in the local range. Overall, the cable force of ZDM is slightly smaller than that of SBM. In Figure 10b,c, all the initial states calculated by the conventional method are at least 62.6% less than the peak vertical displacement without PTF and have at least 47.1% less negative bending moment at the tower beam consolidation (both from ZDM). To a certain extent, it confirms the critical role played by the PTF of cable in adjusting the structure's internal force distribution.

According to the calculation results of the above MEM method, for variable section cable-stayed bridges such as Nanxi River Bridge, the application of the MEM method will result in sudden and uneven local variations of the cable force distribution. In particular, the cable force value closest to the tower position may be too large or even exceed the limit (for Nanxi River Bridge, this is the cable number S1). Among all the tensions of all five methods, the peak force was 10,500 kN for the tension of S1 determined by the MEM method, and the minimum value was 5431 kN determined by the ZDM method.

The initial state determined by the MMM method has the problem of frequent changes in the tensioned side of the main beam and poor uniformity of the cable force. However, the absolute value of the vertical displacement of the main beam is small and the positive and negative values of the bending moment are more uniform. In Figure 10a, the cable force values from S1 to S9 show a variation law of increasing and then decreasing. In Figure 10b, the main beam alignment determined by the MMM method has three inflection points in only one-half of the span, which is the most inflection points among all methods. This is unfavorable for reinforced concrete materials with poor tensile properties. The initial state of the main beam determined by the LFM method is in an intermediate state in all aspects.

In conclusion, for variable-section cable-stay-T-structure combination bridges such as Nanxi River Bridge, the ZDM and SBM methods determine a more excellent initial state, using the corresponding cable force values as the initial state before optimization.

4.1.2. The Influence Matrix

As a structural calculator of bridge-specific software, Midas/Civil solves the influence matrix easily and quickly, as in Pan's work [25], and it was used as a method to implement the cable force adjustment of a tied-arch bridge.

In fact, for the selected objective function and constraints, if the structure is an asymmetric cable-stayed bridge, the influence matrices of the cable force on the vertical displacement of the main girder, the stresses in the upper and lower flange of the main girder, the horizontal displacement of the tower in the longitudinal direction, and the cable force should be calculated separately. Since Nanxi River Bridge is a highly symmetric structure along the longitudinal and transverse directions, the longitudinal horizontal displacements of the bridge towers can be neglected. The influence matrix can be a singular array with all elements having zero values to ensure consistency at this point. In addition, to improve the calculation efficiency, the constraints related to the stress of the main beam are input into the final calibration. The influence matrix of the cable force interaction is shown in Equation (16).

$$[I] = \begin{bmatrix} 0.983 & -0.014 & -0.011 & -0.009 & -0.006 & -0.004 & -0.003 & -0.001 & -0.001 \\ -0.016 & 0.984 & -0.013 & -0.011 & -0.008 & -0.005 & -0.003 & -0.002 & -0.001 \\ -0.015 & -0.015 & 0.986 & -0.012 & -0.009 & -0.006 & -0.004 & -0.002 & -0.001 \\ -0.012 & -0.013 & -0.013 & 0.987 & -0.010 & -0.006 & -0.005 & -0.002 & -0.001 \\ -0.010 & -0.010 & -0.010 & -0.011 & 0.990 & -0.007 & -0.005 & -0.002 & -0.001 \\ -0.007 & -0.007 & -0.007 & -0.008 & -0.008 & 0.993 & -0.005 & -0.003 & -0.001 \\ -0.005 & -0.005 & -0.005 & -0.005 & -0.005 & -0.005 & 0.995 & -0.003 & -0.001 \\ -0.002 & -0.002 & -0.002 & -0.003 & -0.003 & -0.003 & -0.003 & 0.997 & -0.001 \\ -0.001 & -0.001 & -0.001 & -0.001 & -0.001 & -0.001 & -0.001 & -0.001 & 0.999 \end{bmatrix}_{9\times 9} \quad (16)$$

The vertical displacements of all sections of interest are symmetrical in the bridge tower axis. The influence matrix of the diagonal cable on the vertical displacement of the $1/2$ span main girder is a matrix of order 9×40. The influence of the unit cable force on the vertical displacement of the $1/2$ span main girder is, respectively, plotted in Figure 11 for cables S1 to S9.

In Equation (16) and Figure 11, the maximum area of influence of each diagonal cable force on the cable itself and the vertical displacement of the main beam is in the anchorage area of the cable beam. The influence value decreases as the distance from the anchorage point of the cable beam increases.

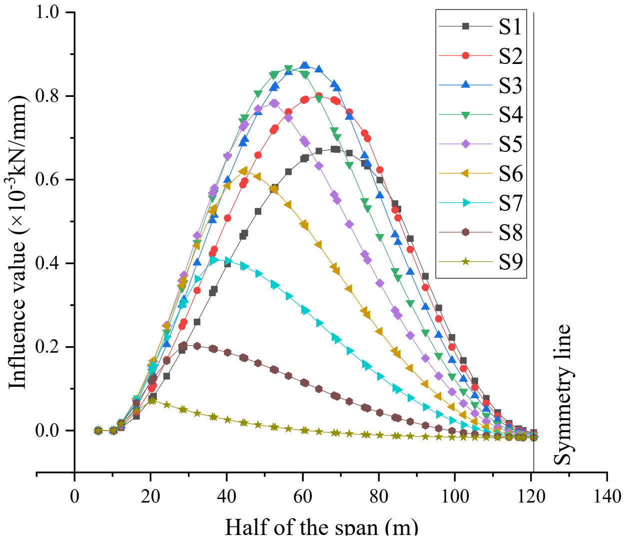

Figure 11. Influence of each cable on the vertical displacement of the main beam.

4.2. Optimization Results and Analysis

The initial states obtained by the ZDM, MEM, SBM, MMM, and LFM methods are optimized separately to obtain the respective sets of individual Pareto front solutions. As an example, the optimization results of the ZDM method are shown in Figure 12.

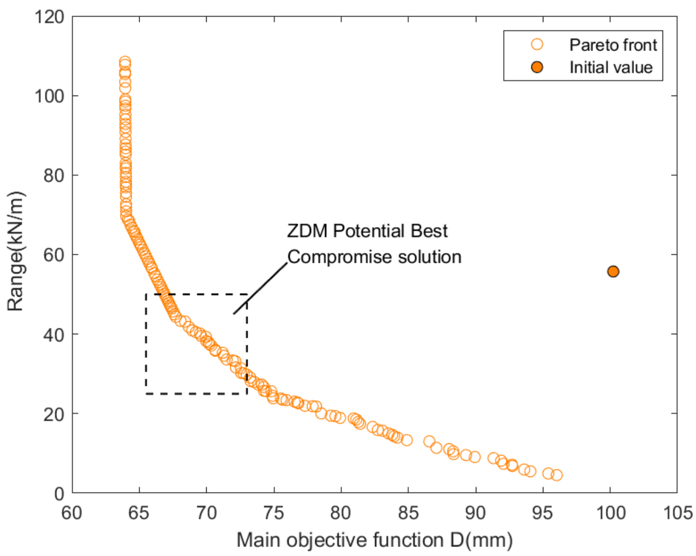

Figure 12. The individual Pareto front solution set of ZDM.

For the Pareto front solution set, the fitness value of the principal objective function D along the horizontal axis increases, but the performance decreases. Similarly, along the vertical axis, the cable force range per unit length R increases, which means that the design target performance decreases. Therefore, in a Pareto front solution set diagram, there are potential optimal compromise solutions in the region that can simultaneously balance the performance of the two design objectives, as shown in the dashed box in Figure 12. There are 34 groups of potential optimal compromise solutions in the individual Pareto front solution set of the ZDM.

In Figure 13, a summary comparison of the Pareto front solution sets optimized by the five initial states is shown. A total of 76 sets of solutions to be selected are boxed by dashed lines, in which there are potentially optimal compromise solutions. Comparing the Pareto front solutions of all methods, the main objective performance of ZDM does not perform well, even for the individual optimal Pareto front solutions of ZDM. The globally optimal Pareto front compromise solution of all methods is the initial optimization result obtained by the SBM calculation.

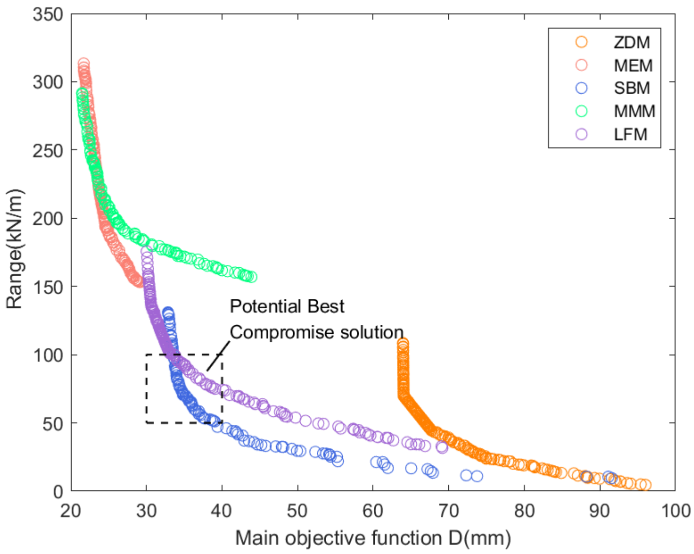

Figure 13. The global Pareto front solution sets.

Fuzzy Set Theory

The above Pareto front solution set contains a series of nondominated solutions, from which the empirically selected solutions cannot reach the global optimum. Abido [26] proposed a fuzzy-set-theory-based approach to extract one of the Pareto optimal solutions as a sound compromising solution and applied it effectively to environmental/economic power dispatch problems. Define membership functions S_i^j:

$$S_i^j = \begin{cases} 1, f_i^j \leq f_i^{\min} \\ \frac{f_i^{\max} - f_i^j}{f_i^{\max} - f_i^{\min}}, f_i^{\min} \leq f_i^j \leq f_i^{\max} \\ 0, f_i^j \leq f_i^{\max} \end{cases} \tag{17}$$

where $f_i^{\max}$ and $f_i^{\min}$ are, respectively, the maximum value and minimum value of the ith optimization objective in the Pareto front solution set; f_i^j and S_i^j are the current value and the affiliation value of the ith optimization objective of the jth solution, respectively.

Define the domination function φ_k,

$$\varphi_k = \frac{\sum_{i}^{2} S_i^k}{\sum_{j=1}^{l} \sum_{i=1}^{2} S_i^j} \tag{18}$$

where l is the number of solutions in the Pareto front solution set. The dominant value of each noninferior solution in the Pareto front solution set can be obtained by calculating φ_k. The dominant value reflects the comprehensive performance of the solution. The solution with larger dominance value is selected as the optimal solution.

The dominance value of the potential optimal compromise solution in the individual Pareto front solution set of ZDM is calculated by the dominance value calculation formula, as shown in Figure 14. The dominance values of each solution for the global potential optimal compromise solution composed of all methods are shown in Figure 15.

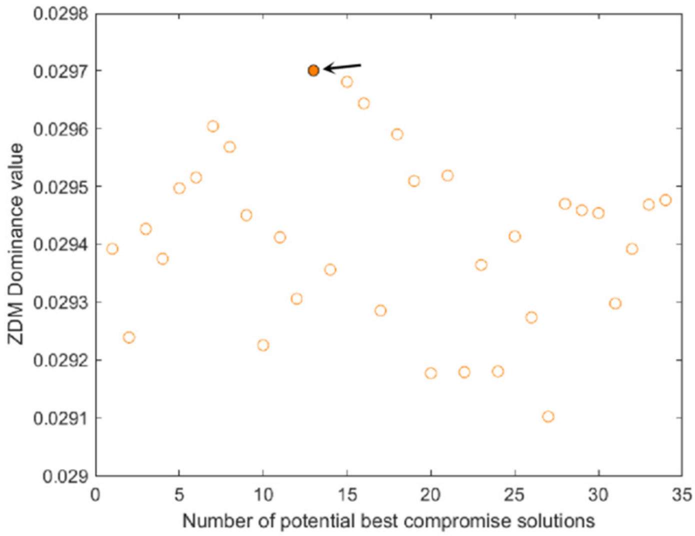

Figure 14. The dominant value of the potential optimal compromise solution of ZDM.

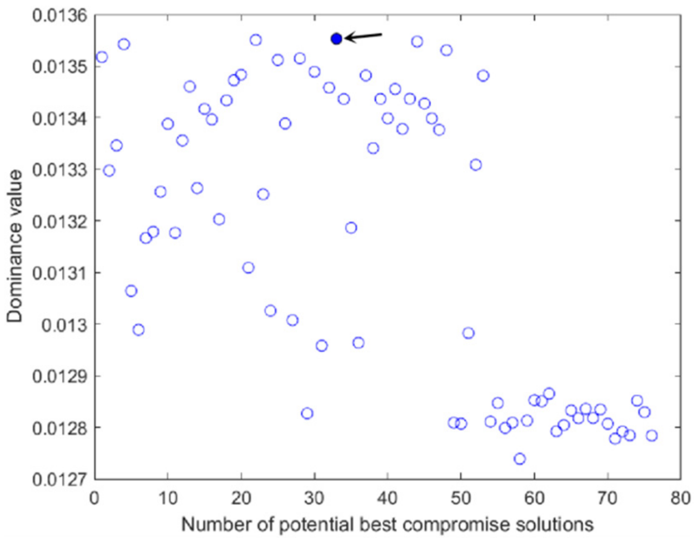

Figure 15. The dominant value of global potential optimal compromise solution.

All orange points in Figure 14 are the dominant values of all Pareto front solutions in the dashed box in Figure 12. The maximum dominance value of the orange solid point pointed by the arrow is the best compromise solution of ZDM. All blue points in Figure 15 are the dominance values of all Pareto front solutions in the dashed box in Figure 13. The maximum dominance value of the blue solid point indicated by the arrow is the global optimal compromise solution.

For the potential optimal compromise solution of ZDM, the maximum dominant value is particle 13, whose dominant value is 0.0297. For the global potential optimal compromise solution, particle 33 has the largest dominant value (0.01355), which comes from the optimization results of the initial state of the SBM. It is worth noting that these two dominant values come from different value intervals and are not comparable. For the optimization objectives of MMM and MEM, the initial state is too unreasonable, so the optimization results are not satisfactory. It is caused by the sensitivity of the SOM to the initial population under the M-MOPSO algorithm kernel. It is shown that when the initial population is too unreasonable, the optimization does not yield reliable results.

Alternatively, the closest alternative to the Pareto optimal compromise solution obtained from the initial state optimization of the SBM is the LFM. LFM methods occupy 23 of the 76 sets of potentially optimal compromise solutions. It shows that if the initial value is within a reasonable range, the result does not depend on the initial value, which is consistent with the findings of Song et al. [22]. In a reasonable range, even if all the cable forces are given the same initial value, a more reliable and reasonable bridge state can be obtained. Experienced bridge designers can estimate the approximate initial range of cable force values based on their experience, and then optimize the cable force to obtain a reasonable bridge condition, which is undoubtedly efficient and exciting. In addition to unreasonable cable force values after optimization, the corresponding design variables of each method after optimization and their values before and after optimization are shown in Table 3.

Table 3. Comparison of cable force values before and after optimization (unit: kN.m).

Number of Stay Cables	S1	S2	S3	S4	S5	S6	S7	S8	S9
ZDM	5431	5440	5379	6090	6293	6212	6834	7533	7969
Optimized value	6139	6800	6724	7613	7866	7765	8543	9416	9961
LFM	7000	7000	7000	7000	7000	7000	7000	7000	7000
Optimized value	6445	7562	8405	9100	9066	9035	9025	8834	9100
Global (from SBM)	5912	6580	6864	6994	7491	7896	8150	8050	8467
Optimized value	7054	8227	8923	9092	9738	10,265	10,571	10,465	11,007

The optimal compromise solution of the global Pareto front solution comes from the initial state determined by the SBM method. The vertical displacement of the main beam, bending moment of the main beam, and axial stress of the cable before and after optimization are shown in Figures 16–18.

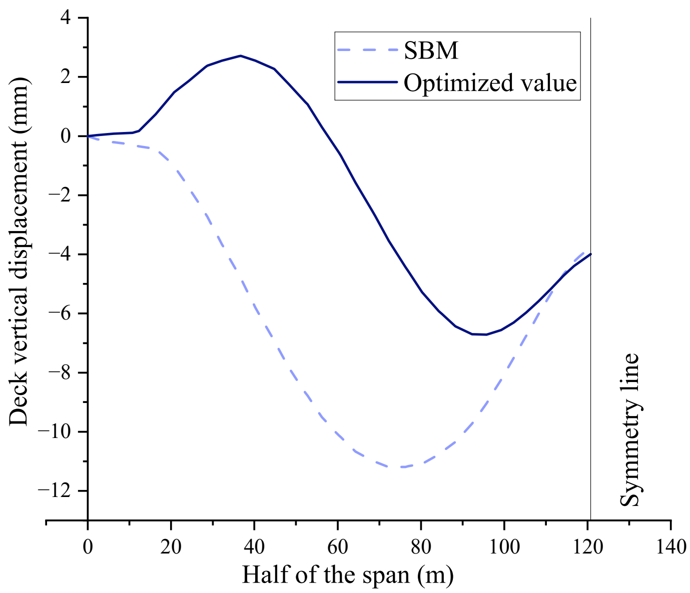

Figure 16. Vertical displacement of the optimized main beam.

In Figure 16, the peak vertical displacement of the optimized main beam is reduced from −11 mm to −6 mm, which is a 45% reduction. The smaller displacement variation means that the alignment of the main beam is smoother and the force is more reasonable under dead load. At the same time, the smaller displacement variation means that the alignment of the main beam is smoother and the force is more reasonable under constant load. In Figure 17, it can be seen that the optimized main beam is subjected to tension on the lower side, which is obviously more conducive to the efficient performance of the mechanical properties of the main beam with tensioned reinforcement configured in the lower part of the neutral axis. The overall stiffness of the combined cable-stayed-T-frame bridge is greater than that of the conventional cable-stayed bridge. Therefore, the huge negative moment at the top of the pier in the tower–girder combination area is the local force state that needs to be focused on. The peak negative bending moments at the top of the pier before and after optimization are −654,971.0 kN.m and −426,875.9 kN.m, respectively, which are reduced by 34.8%. The local force of the optimized main beam is more reasonable.

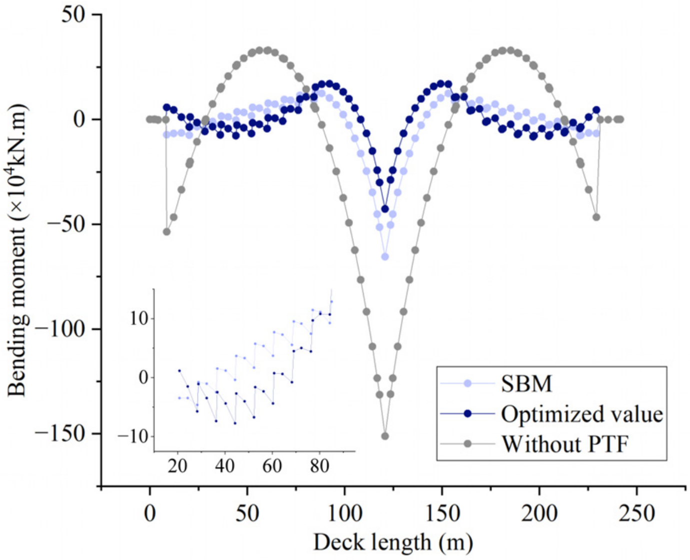

Figure 17. Main beam bending moment before and after optimization.

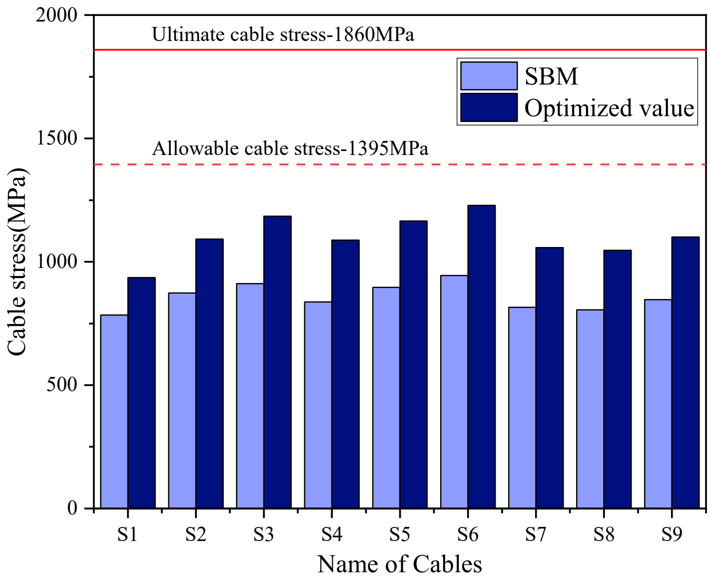

Figure 18. Stress values of cable before and after optimization.

In Figure 18, the optimized cable force values are all increased, which shows that the more rational alignment of the main beam comes at the cost of an increase in cable force. The stress value of each cable is less than the allowable stress value of cable material. The optimized cable force increases with the decrease of the inclination angle, and the cable force varies uniformly from the middle of the span to the root of the tower.

5. Conclusions

In this paper, by incorporating the influence matrix into the M-MOPSO algorithm and establishing a mathematical model, the initial state solution obtained by the traditional method is further optimized to obtain a series of Pareto front solution sets. The fuzzy set theory is then then adopted to select the optimum, and the final reasonable constant load bridge state of the cable-stayed bridge is obtained. The introduced method is validated in the process of solving the reasonable state of a single-tower cable-stayed-T-frame combination bridge. The following conclusions can be drawn from the full study.

(1) The cable force optimization of a cable-stayed bridge can be obtained objectively and accurately by the SOM practical method of fuzzy set theory. Midas/Civil and MATLAB are selected as the structure calculator and cable force optimizer, respectively, and M-MOPSO is used as the calculation kernel to effectively realize the cable force optimization of cable-stayed bridges. This can realize a variety of optimization scheme comparisons, especially suitable for the preliminary design stage.
(2) The optimized cable-stayed bridge has more uniform force and more reasonable alignment. The peak vertical displacement of the optimized main girder is reduced from −11 mm to −6 mm, with a reduction of 45%.
(3) Compared with the classical algorithm NSGA-II, the modified multiobjective particle swarm optimization algorithm with mutation operation (M-MOPSO algorithm) has advantages in both convergence and distribution in dealing with multiobjective problems. It is an effective algorithm for dealing with multiobjective optimization problems.
(4) The M-MOPSO algorithm is influenced by the range of initial tension values, so the SOM method with its kernel has a certain sensitivity to initial populations. Once the initial values are within a reasonable range, even if all the initial values of the diagonal cables are taken to be the same, a more reliable and reasonable bridge state can be obtained.

Author Contributions: Conceptualization, L.W. and Z.X.; methodology, L.W. and Z.X.; software, L.W., Z.X. and M.L.; validation, L.W. and M.L.; formal analysis, Z.X. and L.W.; data curation, M.L.; writing—review and editing, Z.X. and N.F.; project administration, L.W. and N.F.; funding acquisition, L.W. All authors have read and agreed to the published version of the manuscript.

Funding: This study is supported by four key funds: The Key Research and Development Program of Heilongjiang Province, China (JD22A012, GZ20210206); China Railway 22 Bureau Group Co., Ltd. Science and technology research project (20-01A); The Fundamental Research Funds for the Central Universities, China (2572020AW53, 2572019CP02).

Institutional Review Board Statement: This study did not require ethical approval.

Informed Consent Statement: Informed consent was obtained from all subjects involved in the study.

Data Availability Statement: The data presented in this study are available on request from the corresponding author. The data are not publicly available due to privacy.

Conflicts of Interest: The authors declare no conflict of interest.

Nomenclature

C	regulated vector
E	elastic modulus
f_1, f_2	objective functions
f_i^j	current value of the *i*th optimization objective function of the *j*th solution
I	influence matrix
$L_{\rm i}$	length of the *i*th stay cable
n	the number of design variables and the number of optimized cable force values
S_i^j	the membership value of the *i*th optimization objective of the *j*th solution
t	update iterations of particles
$T_{\rm i}$	the *i*th design variable and the *i*th cable force value
X	modulation vector
φ_k	dominant function of the *k*th Pareto front solution

References

1. Liang, P. Practical method of optimization of cable tensions for cable-stayed bridges. *J. Tongji Univ.* **2003**, *31*, 1270–1274.
2. Wang, P.H.; Tseng, T.C.; Yang, C.G. Initial shape of cable-stayed bridges. *Comput. Struct.* **1993**, *47*, 111–123. [CrossRef]

3. Chen, D.W.; Au, F.T.K.; Tham, L.G.; Lee, P.K.K. Determination of initial cable forces in prestressed concrete cable-stayed bridges for given design deck profiles using the force equilibrium method. *Comput. Struct.* **2000**, *74*, 1–9. [CrossRef]
4. Dan, D.; Yang, T. Automatic cable force adjustment for cable stayed bridge based on influence matrix and particle swarm optimization algorithm. *J. Tongji Univ.* **2013**, *41*, 355–360.
5. Xiao, R.C.; Xiang, H.F. Influence matrix method for cable force optimization of cable-stayed bridges. *J. Tongji Univ.* **1998**, *3*, 235–240.
6. Martins, A.M.; Simões, L.M.; Negrão, J.H. Optimization of cable-stayed bridges: A literature survey. *Adv. Eng. Softw.* **2020**, *149*, 102829. [CrossRef]
7. Dai, J.; Qin, F.J.; Di, J.; Chen, Y.R. Review on cable force optimization method for cable-stayed bridge in completed bridge state. *China J. Highw. Transp.* **2019**, *32*, 17–37.
8. Wu, X.; Xiao, R.C. Optimization of cable force for cable-stayed bridges with mixed stiffening girders based on genetic algorithm. *J. Jiangsu Univ.* **2014**, *35*, 722–726.
9. Arellano, H.; Tolentino, D.; Gómez, R. Optimum criss crossing cables in multi-span cable-stayed bridges using genetic algorithms. *KSCE J. Civ. Eng.* **2019**, *23*, 719–728. [CrossRef]
10. Feng, Y.; Lan, C.; Briseghella, B.; Fenu, L.; Zordan, T. Cable optimization of a cable-stayed bridge based on genetic algorithms and the influence matrix method. *Eng. Optim.* **2022**, *51*, 20–39. [CrossRef]
11. Zhu, M.; Liu, R.G.; Xie, G.H.; Cai, D.S. Cable force optimization of long-span cable-stayed bridge based on multi-population genetic algorithm. *World Bridges* **2016**, *46*, 38–42.
12. Birinci, A.; Adıyaman, G.; Yaylacı, M.; Öner, E. Analysis of Continuous and Discontinuous Cases of a Contact Problem Using Analytical Method and FEM. *Lat. Am. J. Solids Struct.* **2015**, *12*, 1771–1789. [CrossRef]
13. Liu, X.S. Determining the Reasonable State of Cable-Stayed Bridges Based on Multi-Objective Particle Swarm Optimization Algorithm. Master's Thesis, Changsha University of Science & Technology, Changsha, China, 2019.
14. Zhang, Y.P.; Liu, X.S.; Li, C.X. Optimization of cable tension of cable-stayed bridges based on multi-objective particle swarm optimization algorithm. *J. Civ. Environ. Eng.* **2020**, *42*, 107–114.
15. Atmaca, B. Size and post-tensioning cable force optimization of cable-stayed footbridge. *Structures* **2021**, *33*, 2036–2049. [CrossRef]
16. Atmaca, B.; Tayfun, D.E.D.E.; Grzywinski, M. Optimization of cables size and prestressing force for a single pylon cable-stayed bridge with Jaya algorithm. *Steel Compos. Struct.* **2020**, *34*, 853–862.
17. Poli, R.; Kennedy, J.; Blackwell, T. Particle swarm optimization. *Swarm Intell.* **2007**, *1*, 33–57. [CrossRef]
18. Liu, Y. Improvements and Application of Particle Swarm Optimization Algorithm. Ph.D. Thesis, Xidian University, Xi'an, China, 2013.
19. Zitzler, E.; Deb, K.; Thiele, L. Comparison of multiobjective evolutionary algorithms: Empirical results. *Evol. Comput.* **2000**, *8*, 173–195. [CrossRef] [PubMed]
20. Zhang, L.W.; Xia, R.J. The reasonable finished dead state research of partially earth-anchored cable-stayed bridge. *Adv. Mater. Res.* **2011**, *255*, 1319–1325. [CrossRef]
21. Sung, Y.C.; Chang, D.W.; Teo, E.H. Optimum post-tensioning cable forces of Mau-Lo Hsi cable-stayed bridge. *Eng. Struct.* **2006**, *28*, 1407–1417. [CrossRef]
22. Song, C.; Xiao, R.; Sun, B. Optimization of cable pre-tension forces in long-span cable-stayed bridges considering the counterweight. *Eng. Struct.* **2018**, *172*, 919–928. [CrossRef]
23. Zhang, H.H.; Sun, N.N.; Wang, P.Z.; Liu, M.H.; Li, Y. Optimization of Cable Force Adjustment in Cable-Stayed Bridge considering the Number of Stay Cable Adjustment. *Adv. Civ. Eng.* **2020**, *2020*, 1–20. [CrossRef]
24. Chen, Z.J.; Liu, Y.; Yang, L.F.; Zhang, S.B. Optimization of stay cable tension of completed bridge of single-pylon cable-stayed bridge based on particle swarm optimization algorithm. *Bridge Constr.* **2016**, *46*, 40–44.
25. Pan, G.M. Implementation of influence matrix in cable force adjustment in MIDAS/CIVIL. *Sci. Technol. Eng.* **2011**, *11*, 6763–6766.
26. Abido, M.A. Multi-objective evolutionary algorithms for electric power dispatch problem. *IEEE Trans. Evol. Comput.* **2006**, *10*, 315–329.